PHYSICAL REVIEW B VOLUME 57, NUMBER 11 15 MARCH 1998-I

Correlation between atomic-scale structure and mobility anisotropy in $InAs/Ga_{1-x}In_xSb$ superlattices

A. Y. Lew,* S. L. Zuo, and E. T. Yu†
Department of Electrical and Computer Engineering, University of California at San Diego, La Jolla, California 92093-0407

R. H. Miles‡
Hughes Research Laboratories, 3011 Malibu Canyon Road, Malibu, California 90265

(Received 28 July 1997)

We have performed detailed characterization of atomic-scale interface structure in $InAs/Ga_{1-x}In_xSb$ superlattices using cross-sectional scanning tunneling microscopy (STM) and established a semiquantitative correlation between interface structure and transport properties in these structures. Quantitative analysis of STM images of both (110) and $(1\bar{1}0)$ cross-sectional planes of the superlattice indicates that interfaces in the $(1\bar{1}0)$ plane exhibit a higher degree of interface roughness than those in the (110) plane and that the $Ga_{1-x}In_xSb$-on-InAs interfaces are rougher than the InAs-on-$Ga_{1-x}In_xSb$ interfaces. The roughness data are consistent with anisotropy in interface structure arising from anisotropic island formation during growth and, in addition, a growth-sequence-dependent interface structure arising from differences in interfacial bond structure between the two interfaces. Low-temperature Hall measurements performed on these samples demonstrate the existence of a substantial lateral anisotropy in mobility that is in semiquantitative agreement with modeling of interface roughness scattering that incorporates our quantitative measurements of interface roughness using STM. [S0163-1829(98)03911-3]

I. INTRODUCTION

$InAs/Ga_{1-x}In_xSb$ strained-layer superlattices have shown great promise for application in mid- to long-wavelength infrared imaging applications,[1,2] and have been used successfully as the active layers in both photodiodes[3] and diode lasers.[4] However, the atomic-scale interfacial properties of these superlattice structures have been found to be of crucial importance in determining material and device properties. Because both group-III and group-V constituents change from one superlattice layer to the next, two distinct bond configurations—InSb-like and $Ga_{1-x}In_xAs$-like—can be present at each interface.[5] $Ga_{1-x}In_xSb$/InAs superlattices grown with InSb-like interfacial bonds are expected to possess superior device characteristics compared to those grown with $Ga_{1-x}In_xAs$-like bonds,[6,7] and studies of transport in InAs/AlSb quantum wells have shown that higher mobilities can be achieved when the structures are grown with InSb-like interfaces than with AlAs-like interfaces.[8] A detailed understanding of the atomic-scale structural and compositional properties of these interfaces, and the relationship between these material properties and various aspects of device performance, is therefore essential to the optimization of electrical and optical properties of device structures based on the $InAs/Ga_{1-x}In_xSb$ and related material systems.

In this paper we describe a detailed, quantitative analysis of interface structure in $InAs/Ga_{1-x}In_xSb$ superlattices using cross-sectional scanning tunneling microscopy (STM) and semiquantitative correlation of these STM results with measurements of low-temperature Hall mobilities. High-resolution cross-sectional STM imaging of the $InAs/Ga_{1-x}In_xSb$ superlattices allows atomic-scale interface roughness and asymmetry to be profiled directly, and is used to investigate directly and quantitatively the nature and degree of lateral anisotropy and growth-sequence dependence in interface structure. Features in interface structure revealed by our analysis are interpreted as consequences of anisotropy in island formation during sample growth and of differences in growth-sequence-dependent bond configuration at the interfaces. We also present the results of low-temperature Hall mobility studies performed on the superlattice samples. The Hall mobilities are found to be highly anisotropic, and modeling of interface roughness scattering using the interface roughness data derived from high-resolution STM images demonstrates a semiquantitative correlation between the measured Hall mobility anisotropy and quantitative measurements of interface roughness obtained by STM.

II. EXPERIMENT

The $InAs/Ga_{1-x}In_xSb$ superlattice sample used in this study was grown by solid-source molecular-beam epitaxy (MBE) in a VG V80 MKII MBE system on an n-type GaSb (001) substrate. The growth system and substrate preparation techniques have been described in detail elsewhere.[9] The superlattice consisted of 50 Å $Ga_{0.75}In_{0.25}Sb$ alternating with 17 Å InAs for 150 periods, capped with 500 Å GaSb. The epitaxial layers were grown at 380 °C on a 1000-Å GaSb buffer layer. At each interface in the superlattice layers, a 5-sec Sb soak was used to induce the formation of InSb-like bonds. The average composition and overall structural quality of the superlattice were confirmed by high-resolution x-ray diffraction.

STM experiments were conducted in an ultrahigh-vacuum system at a base pressure of approximately 1–2 $\times 10^{-10}$ Torr. Superlattice samples were cleaved *in situ* to expose either a (110) or a $(1\bar{1}0)$ cross-sectional face on

 © 1998 The American Physical Society

which STM imaging was performed. While atomically flat cross-sectional surfaces were obtained for both the (110) and $(1\bar{1}0)$ planes, we found that cleaving to expose the (110) surface was generally more successful. Both Pt-Ir and W tips cleaned *in situ* by electron bombardment were used for these studies. Because the cleaved surfaces are atomically flat, the contrast seen in constant-current STM images corresponds primarily to features in the electronic structure of the sample, rather than to the actual physical topography of the surface. For the mobility studies, Hall bars were fabricated using standard photolithography and wet-etching techniques. The bars were oriented such that the Hall voltages were measured along both the $[1\bar{1}0]$ and $[110]$ directions. Measurements were obtained in a variable-temperature Hall measurement apparatus over a wide range of applied currents and magnetic fields.

III. INTERFACE ROUGHNESS STUDIES

Previous cross-sectional STM studies of InAs/GaSb (Refs. 10–12) and InAs/$Ga_{0.75}In_{0.25}Sb$ (Refs. 13 and 14) superlattices have provided considerable evidence of interface roughness and growth-sequence-dependent interface asymmetry. For InAs/$Ga_{0.75}In_{0.25}Sb$ structures, interfaces in which $Ga_{0.75}In_{0.25}Sb$ was grown on InAs typically appear more abrupt electronically in cross-sectional STM images than interfaces in which InAs was grown on $Ga_{0.75}In_{0.25}Sb$,[13] and measurements of orbital spacings obtained from STM images suggested a greater degree of InSb-like character at the InAs-on-$Ga_{0.75}In_{0.25}Sb$ interfaces.[14] Furthermore, x-ray-diffraction and simulation studies by Miles *et al.* have suggested an asymmetry in interface structure in InAs/$Ga_{1-x}In_xSb$ superlattices, even under growth conditions intended to produce entirely InSb-like interfaces.[9] These studies suggested that the $Ga_{1-x}In_xSb$ layers are terminated with InSb-like bonds, while the InAs layers are terminated by roughly equal numbers of InSb-like and $Ga_{1-x}In_xAs$-like bonds. In this work, a more detailed, quantitative analysis of interface roughness and growth-sequence dependence of interface asymmetry has been performed using cross-sectional STM, and the resulting quantification of atomic-scale interface structure has been correlated with low-temperature measurements of Hall carrier mobility.

Figure 1 shows a high-resolution constant-current cross-sectional image of the InAs/$Ga_{0.75}In_{0.25}Sb$ superlattice structure, obtained at a sample bias voltage of −1.5 V and a tunneling current of 0.1 nA. The contrast between the darker InAs layers and the brighter $Ga_{0.75}In_{0.25}Sb$ layers is clearly visible. This contrast is electronically induced, rather than arising from features in the actual physical topography of the cleaved surface. For negative sample bias voltage and at a given tip-sample separation, both the band offsets and the expected distribution of carriers in the InAs/$Ga_{0.75}In_{0.25}Sb$ superlattice would lead to increased tunneling current in the $Ga_{0.75}In_{0.25}Sb$ layers as compared to the InAs layers, giving rise to apparent topographic features in a constant-current image. Also evident in the image is monolayer-level roughness between the InAs and $Ga_{0.75}In_{0.25}Sb$ layers. A large number of images of similar quality were obtained over regions up to 1000 Å×1000 Å in size from both (110) and $(1\bar{1}0)$ cross sections of the sample. All images showed a

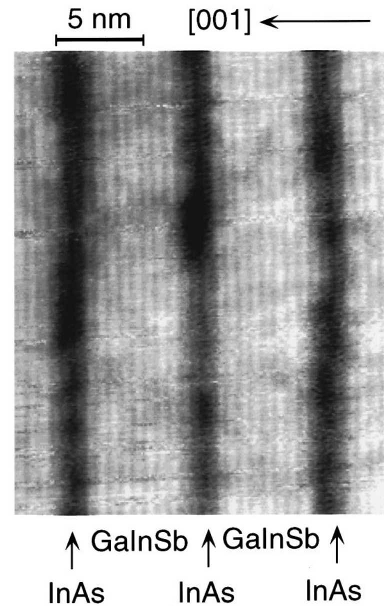

FIG. 1. High-resolution constant-current STM image of a 50-Å $Ga_{0.75}In_{0.25}Sb$/17-Å InAs superlattice, obtained at a sample bias of −1.5 V and a tunneling current of 0.1 nA. The gray-scale range of the image is 2.5 Å. Monolayer roughness is visible at the interfaces between the InAs layers and $Ga_{0.75}In_{0.25}Sb$ layers.

clear contrast between the InAs layers and the $Ga_{0.75}In_{0.25}Sb$ layers, as well as evidence of monolayer-level interface roughness.

Individual interface profiles were extracted from the images by enhancing the contrast between the InAs and $Ga_{0.75}In_{0.25}Sb$ layers and then using an edge-detection algorithm to delineate the interfaces. Profiles were compared to the original images to ensure that accurate representations of the interfaces were obtained. Quantitative interface profiles $a(x)$ were obtained by measuring the distance between the interfaces and a baseline corresponding to the profile of the atomic bilayers in the image from which the interfaces have been extracted. Figure 2 shows representative interface pro-

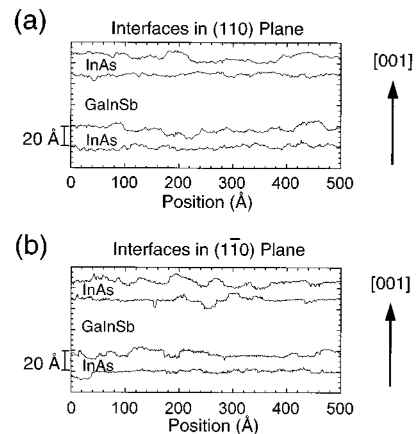

FIG. 2. Representative interface profiles obtained from (a) (110) and (b) $(1\bar{1}0)$ cross-sectional STM images of the 50-Å $Ga_{0.75}In_{0.25}Sb$/17-Å InAs superlattice sample. The [001] growth direction is indicated.

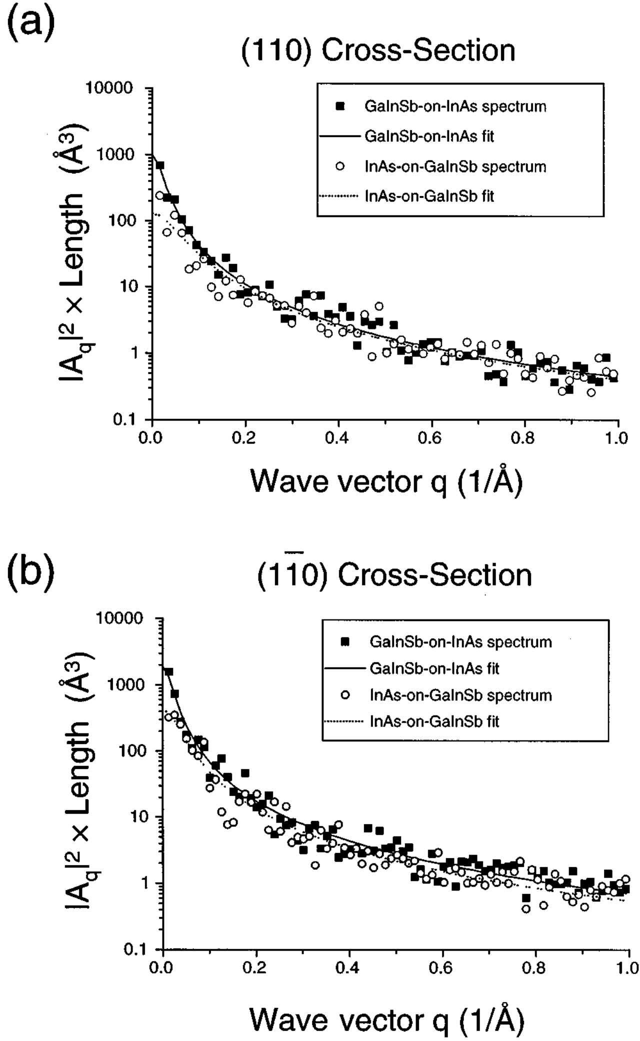

FIG. 3. Interface roughness power spectra (symbols) and Lorentzian fits to the spectra (lines) for $Ga_{0.75}In_{0.25}Sb$-on-InAs and InAs-on-$Ga_{0.75}In_{0.25}Sb$ interfaces from (a) (110) and (b) $(1\bar{1}0)$ cross sections of the superlattice. Roughness amplitudes and correlation lengths for each interface type are listed in Table I.

files extracted from high-resolution constant-current STM images similar in quality to that of Fig. 1. In total, several dozen interface profiles, each 500 Å in length, were extracted from multiple STM images of both (110) and $(1\bar{1}0)$ cross-sectional surfaces.

The roughness spectra of the interfaces were calculated by taking discrete Fourier transforms of the extracted profiles. The roughness frequency components A_q are given by

$$A_q=\frac{2}{N}\sum_{n=0}^{N-1} a(nd)e^{-iqd}, \tag{1}$$

where $q=2\pi n/L$, L is the length of the interface, and d is the spacing between data points along the interface (typically 0.5 Å). The roughness power spectrum of each interface, $|A_q|^2$, is fitted to a Lorentzian function

$$|A_q|^2=\frac{1}{L}\frac{2\Delta^2(\Lambda/2\pi)}{1+(q\Lambda/2\pi)^2}, \tag{2}$$

TABLE I. Roughness amplitudes and correlation lengths obtained from fitting a Lorentzian function to the interface roughness power spectra calculated for $Ga_{0.75}In_{0.25}Sb$-on-InAs and InAs-on-$Ga_{0.75}In_{0.25}Sb$ interfaces from (110) and $(1\bar{1}0)$ cross-sectional images.

Cross section	Interface	Amplitude Δ (Å)	Correlation length Λ (Å)
$(1\bar{1}0)$	$Ga_{1-x}In_xSb$-on-InAs	4.3±0.2	327±38
$(1\bar{1}0)$	InAs-on-$Ga_{1-x}In_xSb$	2.8±0.2	174±21
(110)	$Ga_{1-x}In_xSb$-on-InAs	3.2±0.2	301±39
(110)	InAs-on-$Ga_{1-x}In_xSb$	1.9±0.1	112±16

where Δ is the roughness amplitude and Λ the roughness correlation length. We find the Lorentzian to be a better fit to our data than a Gaussian or other functional forms. The Lorentzian spectral distribution corresponds to an exponential correlation in real space and is the spectral distribution expected for a random spatial distribution of steps at the interface.[15] The analysis described here is similar to that used by other workers to quantify interface roughness measured by cross-sectional STM.[10,11,16,17] Figure 3 shows a plot of the power spectra and also of Lorentzian fits to the power spectra for the $Ga_{1-x}In_xSb$-on-InAs and InAs-on-$Ga_{1-x}In_xSb$ interfaces from both (110) and $(1\bar{1}0)$ cross sections. Table I lists the extracted roughness parameters for each interface type. The spectra shown are averages of individual roughness spectra from at least six different profiles for each interface type.

As indicated in Table I, the interfaces in the $(1\bar{1}0)$ plane exhibit larger roughness amplitudes and correlation lengths than those in the (110) plane. This observation is consistent with reflection high-energy electron-diffraction[18] (RHEED) and STM (Refs. 19 and 20) studies of growth of (001) GaAs by MBE, in which islands and terraces on the GaAs surface were observed to be elongated in the $[1\bar{1}0]$ direction. Islands elongated in the $[1\bar{1}0]$ direction have also been seen in STM studies of GaSb grown on InAs surfaces for both GaAs-like and InSb-like interfaces.[12] Similar island formation during growth of the InAs/$Ga_{1-x}In_xSb$ layers would lead to a corresponding anisotropy in interface structure. Interface structure in the (110) plane would reflect the presence of the more elongated island cross sections present along the $[1\bar{1}0]$ direction; for a given interface length along the $[1\bar{1}0]$ direction, the interface structure observed would be influenced by a smaller number of island and terrace steps, leading to smaller amplitude components in the roughness spectrum. Interface structure in the $(1\bar{1}0)$ plane, conversely, would reflect the presence of the shorter, transverse-island cross sections found along the [110] direction; for a given interface length along the [110] direction, the interface structure seen would be influenced by a larger number of island and terrace steps than for the $[1\bar{1}0]$ direction, leading to increased interface roughness. The quantitative results obtained from our interface roughness analysis are consistent with this interpretation.

The parameters in Table I also show a substantial depen-

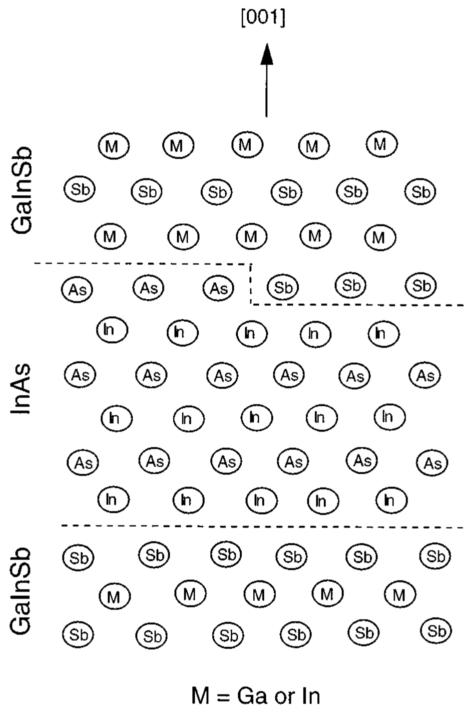

FIG. 4. Schematic diagram of an InSb-like interface structure at the InAs-on-$Ga_{1-x}In_xSb$ interface, and a mixed InSb-like and $Ga_{1-x}In_xAs$-like interface structure at the $Ga_{1-x}In_xSb$-on-InAs interface in an InAs/$Ga_{1-x}In_xSb$ superlattice. The dashed lines indicate the positions of the interfaces. The [001] growth direction is indicated. Since STM is sensitive to the electronic properties of atomic-scale interface structure, the differences in roughness at the two different interfaces would be reflected in the STM data.

dence of interface roughness on growth sequence, with the $Ga_{1-x}In_xSb$-on-InAs interfaces being substantially rougher than the InAs-on-$Ga_{1-x}In_xSb$ interfaces. In earlier studies of InAs/GaSb superlattices using STM, a substantial dependence of interface structure on growth sequence was observed, with the degree of asymmetry observed in interface structure dependent upon the growth conditions employed.[10–12] Furthermore, x-ray-diffraction analyses of InAs/$Ga_{1-x}In_xSb$ superlattice samples have suggested that the $Ga_{1-x}In_xSb$ layers are terminated with InSb-like bonds, while the InAs layers are terminated by roughly equal numbers of InSb-like and $Ga_{1-x}In_xAs$-like bonds.[9] The $Ga_{1-x}In_xSb$-on-InAs interfaces would then be of mixed InSb-like and $Ga_{1-x}In_xAs$-like character, while the InAs-on-$Ga_{1-x}In_xSb$ interfaces would be of a more homogenous InSb-like character. As shown schematically in Fig. 4, mixed stoichiometry at one interface will lead to increased atomic-scale roughness at that interface. The roughness data obtained from our STM measurements are consistent with this—the $Ga_{1-x}In_xSb$-on-InAs interfaces, at which mixed stoichiometry is expected to be present, are measurably rougher than the InAs-on-$Ga_{1-x}In_xSb$ interfaces, for which we expect the stoichiometry to be more uniform.

IV. CORRELATION TO MOBILITY STUDIES

The results of the preceding interface roughness analysis have been correlated to data obtained from low-temperature

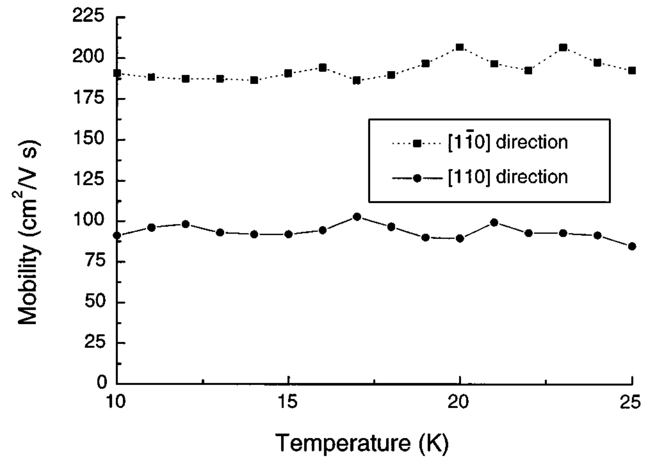

FIG. 5. Measured Hall mobilities for the superlattice as functions of temperature and direction. The mobility is observed to be larger in the $[1\bar{1}0]$ direction than in the [110] direction of the superlattice.

Hall measurements of mobility. Magnetotransport measurements have shown that mobility in InAs/$Ga_{1-x}In_xSb$ superlattices is dominated by interface roughness scattering for temperature regimes of interest for long-wavelength infrared devices (4.2–200 K).[21,22] In our studies, temperature-dependent mobilities were measured for transport along both the [110] and $[1\bar{1}0]$ directions of the superlattice. Although the sample used in this study was grown on an n-type substrate in order to facilitate STM measurements, mobility measurements obtained at temperatures below the GaSb freeze-out temperature are expected to correspond primarily to conduction within the superlattice epitaxial layers. Assuming a Te dopant concentration of $\sim 3.2\times 10^{17}$ cm^{-3} in GaSb and a binding energy of 10 meV,[23] the freeze-out temperature is predicted to be 23 K. Previous temperature-dependent Hall mobility measurements performed on samples consisting of 75-period superlattice structures nominally identical to the samples used in the studies reported here, but grown on GaSb buffer layers on semi-insulating GaAs substrates, revealed a clear anisotropy in the carrier mobility, with the mobility being larger in the $[1\bar{1}0]$ direction than in the [110] direction.[24] Furthermore, transport measurements obtained by growing InAs/Al,GaSb quantum wells on lattice-matched GaSb substrates have been shown to be similar to those obtained by growing the quantum wells on GaSb buffer layers on GaAs substrates.[25] Anisotropic low-temperature Hall mobilities have also been observed in modulation-doped $Al_xGa_{1-x}As$/GaAs heterostructures grown by MBE.[26] In these studies, mobility in the $[\bar{1}10]$ direction was measured to be larger than that in the [110] direction and was attributed to scattering from interface islands longer in the $[\bar{1}10]$ direction than in the [110] direction.

Figure 5 shows the measured p-type Hall mobility for the superlattice sample. The mobility at low temperature is observed to be larger in the $[1\bar{1}0]$ direction than in the [110] direction of the superlattice by a factor of approximately 1.5–2. At higher temperatures than those shown in the figure, carrier transport is dominated by the substrate: the carrier mobilities reach values similar to those seen in measure-

ments performed using n-type GaSb[27] and the mobility ratio reaches unity. The measured values of the carrier mobility shown in Fig. 5 are smaller than those observed in studies of superlattice samples with 25-Å $Ga_{0.75}In_{0.25}Sb$ and ≥25-Å InAs layers.[21,22] However, this can be explained by considering the dependence of interface-roughness-limited mobility on the well widths of the structures. Interface roughness scattering in a quantum well with thick, infinitely high barriers leads to an expected mobility dependence on the well width d of $\mu \propto d^6$,[28] while the measured dependence of the low-temperature carrier mobility on layer width was $\mu \propto d^{2.4}$.[21] Using the reported mobility of 3900 cm^2/V sec for a 25-Å InAs well in an n-type InAs/$Ga_{0.75}In_{0.25}Sb$ superlattice, an extrapolation of the mobility using either a $\mu \propto d^{2.4}$ or a $\mu \propto d^6$ dependence on well width results in values of Hall mobilities for our sample structure that are within reasonable range of our measurements.

A rough estimate of the mobility anisotropy ratio based on interface roughness scattering relaxation times may be obtained using the extracted roughness parameters from the STM data. In this calculation, the matrix element for scattering $S(q)$ is proportional to the Fourier transform of the distribution of steps at each interface. Assuming the dependence of energy on well widths to be the same for both spatial directions, we take the interface roughness dependence of $S(q)$ to be given by the Fourier transform of the autocorrelation of the interface profiles.[15] However, this is just given by Eq. (2), the Lorentzian which is fitted to the power spectrum of each interface. $S(q)$ is then incorporated into the momentum relaxation time $\tau(k)$ using the relation

$$\frac{1}{\tau(k)}=\frac{e^2F_s^2m^*}{2\pi\hbar^3}\int_0^{2\pi}d\theta(1-\cos\,\theta)S(q)\left[\frac{\Gamma(q)}{\varepsilon(q)}\right]^2,$$

$$q=2k\,\sin\,\theta/2, \tag{3}$$

where F_s is the average surface field, m^* is the effective mass parallel to the interface, k is the electron wave vector, θ is the scattering angle, $\Gamma(q)$ contains corrections for image potential and electric field modification at the deformed interface, and $\varepsilon(q)$ is the electron dielectric function to account for free-electron screening. The drift mobility is related directly to the scattering times by[28]

$$\mu=\frac{e}{m^*}\langle\tau\rangle. \tag{4}$$

Assuming a Hall scattering factor of 1, the Hall mobility and drift mobility may be taken to be equal. Using Eqs. (3) and (4) and the roughness parameters given in Table I, the ratio of interface roughness scattering times for transport in the $[1\bar{1}0]$ and $[110]$ directions, $\tau[1\bar{1}0]/\tau[110]$, is calculated numerically as a function of k. Total scattering times associated with each direction are calculated from the scattering times from the individual interface types according to the expression

$$\frac{1}{\tau_{\text{total}}}=\frac{1}{\tau_{\text{GaInSb-on-InAs}}}+\frac{1}{\tau_{\text{InAs-on-GaInSb}}}. \tag{5}$$

Figure 6 shows a plot of the calculated scattering time ratios vs k. These calculations confirm that the scattering relaxation times for interfaces in the $[1\bar{1}0]$ direction are longer than those in the $[110]$ direction; furthermore, the ratio of the scattering times is in semiquantitative agreement with the actual measured mobility ratio of the superlattice sample. The estimates indicate that a mobility anisotropy of more than a factor of 2 can be expected for wave vectors k of ~0.08 $Å^{-1}$ or smaller, corresponding to carrier scattering from features in the heterojunction interface structure with characteristic lateral sizes of ~75 Å or greater.

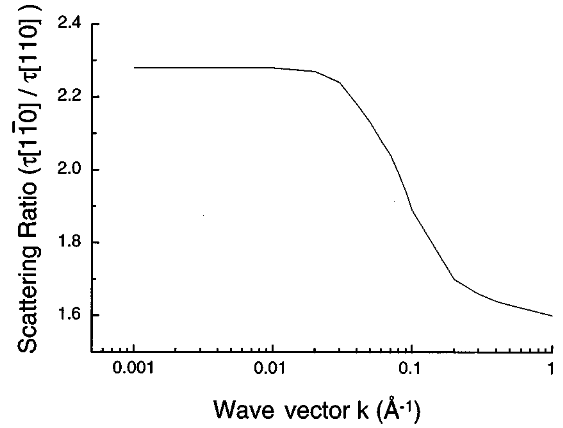

FIG. 6. Calculated ratio of interface roughness scattering times as a function of k using the interface roughness parameters determined by STM for the 17-Å InAs/50-Å $Ga_{0.75}In_{0.25}Sb$ superlattice. The scattering time ratios should be directly proportional to the carrier mobility ratios in the superlattice. The anisotropy in the calculated scattering times is in semiquantitative agreement with the measured anisotropy in Hall mobility in the superlattice.

While the above calculation provides a rough estimate of the influence of anisotropic interface roughness on mobility, it should be noted that the carrier mobility is highly dependent on the band structure of the superlattice, and the band structure itself is sensitive to fluctuations in the confinement energy caused by interface roughness (i.e., spatial variation of the widths of both wells and barriers). A detailed analysis of the mobility in these superlattices would therefore need to incorporate both detailed interface roughness information such as that obtained in our STM measurements and a realistic calculation of the superlattice electronic structure and its influence on transport properties. Such an analysis is a subject of current investigation. Nevertheless, our studies described here demonstrate semiquantitative agreement between the atomic-scale electronic and structural anisotropy directly observed by cross-sectional STM and macroscopic carrier transport data obtained using devices fabricated from the same samples.

V. CONCLUSIONS

We have used cross-sectional STM to investigate directly and quantitatively the atomic-scale interface morphology of InAs/$Ga_{1-x}In_xSb$ superlattices grown by MBE, and have demonstrated a semiquantitative correlation between atomic-scale interface structure and transport properties in these structures. Spectral analysis of interface profiles obtained by STM shows that interfaces in the $(1\bar{1}0)$ cross-sectional plane

have larger roughness amplitudes and correlation lengths than those in the (110) cross-sectional plane; this directional anisotropy in the interface structure of the superlattice layers is interpreted as a consequence of anisotropic island formation during growth. The roughness spectra also indicate the presence of a growth-sequence-dependent interface structure: interfaces in which $Ga_{1-x}In_xSb$ has been grown on InAs are substantially rougher than interfaces in which InAs has been grown on $Ga_{1-x}In_xSb$. This dependence is interpreted as arising from differences in interfacial bond structure produced under various growth conditions and supports earlier observations suggesting a more homogenous InSb-like bond character at the InAs-on-$Ga_{1-x}In_xSb$ interfaces than at the $Ga_{1-x}In_xSb$-on-InAs interfaces. Hall mobilities measured below the freeze-out temperature of the GaSb substrate reveal a marked anisotropy in mobility, with the mobility being higher in the $[1\bar{1}0]$ direction than in the [110] direction in the superlattice. Since the interfaces in the $(1\bar{1}0)$ cross-sectional STM images display lower roughness amplitudes and correlation lengths, and correspond to the interfaces along the [110] superlattice direction, the transport anisotropy observed in the Hall mobility measurements correlates with the directional structural anisotropy seen in the STM data. Modeling of the interface roughness scattering times using interface roughness data from our STM studies demonstrates semiquantitative agreement between the atomic-scale electronic and structural anisotropy directly observed by cross-sectional STM and macroscopic carrier transport data obtained from the same device structures.

ACKNOWLEDGMENTS

A.Y.L., S.L.Z., and E.T.Y. would like to acknowledge support from the Hughes Aircraft Company via the UC MICRO program, and the National Science Foundation (Contract Nos. ECS93-07986 and ECS95-01469). E.T.Y. would like to acknowledge financial support from the Alfred P. Sloan Foundation.

*Present address: Motorola MOS10, 1 Banting Drive, Irvine, CA 92618.
†Electronic address: ety@ece.ucsd.edu
‡Present address: SDL, Inc., 80 Rose Orchard Way, San Jose, CA 95134-1365.

[1] D. L. Smith and C. Mailhiot, J. Appl. Phys. **62**, 2545 (1987).
[2] D. H. Chow, R. H. Miles, J R. Söderström, and T. C. McGill, Appl. Phys. Lett. **56**, 1418 (1990).
[3] J. L. Johnson, L. A. Samoska, A. C. Gossard, J. L. Merz, M. D. Jack, G. R. Chapman, B. A. Baumgratz, K. Kosai, and S. M. Johnson, J. Appl. Phys. **80**, 1116 (1996).
[4] T. C. Hasenberg, D. H. Chow, A. R. Kost, R. H. Miles, and L. West, Electron. Lett. **31**, 275 (1995).
[5] I. Sela, I. H. Campbell, B. K. Laurich, D. L. Smith, L. A. Samoska, C. R. Bolognesi, A. C. Gossard, and H. Kroemer, J. Appl. Phys. **70**, 5608 (1991).
[6] D. H. Chow, R. H. Miles, and A. T. Hunter, J. Vac. Sci. Technol. B **10**, 888 (1992).
[7] R. H. Miles, J. N. Schulman, D. H. Chow, and T. C. McGill, Semicond. Sci. Technol. **8**, S102 (1993).
[8] G. Tuttle, H. Kroemer, and J. H. English, J. Appl. Phys. **67**, 3032 (1990).
[9] R. H. Miles, D. H. Chow, and W. J. Hamilton, J. Appl. Phys. **71**, 211 (1992).
[10] R. M. Feenstra, D. A. Collins, D. Z.-Y. Ting, M. W. Wang, and T. C. McGill, J. Vac. Sci. Technol. B **12**, 2592 (1994).
[11] R. M. Feenstra, D. A. Collins, D. Z.-Y. Ting, M. W. Wang, and T. C. McGill, Phys. Rev. Lett. **72**, 2749 (1994).
[12] P. M. Thibado, B. R. Bennett, M. E. Twigg, B. V. Shanabrook, and L. J. Whitman, Appl. Phys. Lett. **67**, 3578 (1995).
[13] A. Y. Lew, E. T. Yu, D. H. Chow, and R. H. Miles, Appl. Phys. Lett. **65**, 201 (1994).
[14] A. Y. Lew, E. T. Yu, D. H. Chow, and R. H. Miles, in *Compound Semiconductor Epitaxy*, edited by C. W. Tu, L. A. Kolodziejski, and V. R. McCrany, MRS Symposium Proceedings No. 340 (Materials Research Society, Pittsburgh, 1994), p. 237.
[15] S. M. Goodnick, D. K. Ferry, C. W. Wilmsen, Z. Liliental, D. Fathy, and O. L. Krivanek, Phys. Rev. B **32**, 8171 (1985).
[16] S. L. Skala, W. Wu, J. R. Tucker, J. W. Lyding, A. Seabaugh, E. A. Beam III, and D. Jovanovic, J. Vac. Sci. Technol. B **13**, 660 (1995).
[17] W. Wu, S. L. Skala, J. R. Tucker, J. W. Lyding, A. Seabaugh, E. A. Beam III, and D. Jovanovic, J. Vac. Sci. Technol. A **13**, 602 (1995).
[18] P. R. Pukite, G. S. Petrich, S. Batra, and P. I. Cohen, J. Cryst. Growth **95**, 269 (1989).
[19] E. J. Heller and M. G. Lagally, Appl. Phys. Lett. **60**, 2675 (1992).
[20] V. Bressler-Hill, R. Maboudian, M. Wassermeier, X.-S. Wang, K. Pond, P. M. Petroff, and W. H. Weinberg, Surf. Sci. **287/288**, 514 (1993).
[21] C. A. Hoffman, J. R. Meyer, E. R. Youngdale, F. J. Bartoli, and R. H. Miles, Appl. Phys. Lett. **63**, 2210 (1993).
[22] C. A. Hoffman, J. R. Meyer, E. R. Youngdale, F. J. Bartoli, R. H. Miles, and L. R. Ram-Mohan, Solid-State Electron. **37**, 1203 (1994).
[23] J. F. Chen and A. Y. Cho, J. Appl. Phys. **70**, 277 (1991).
[24] R. H. Miles (unpublished).
[25] H.-R. Blank, M. Thomas, K. C. Wong, and H. Kroemer, Appl. Phys. Lett. **69**, 2080 (1996).
[26] Y. Tokura, T. Saku, S. Tarucha, and Y. Horikoshi, Phys. Rev. B **46**, 15 558 (1992).
[27] A. Baraldi, F. Colonna, C. Ghezzi, R. Magnanini, A. Parisini, L. Tarricone, A. Bosacchi, and S. Franchi, Semicond. Sci. Technol. **11**, 1656 (1996).
[28] H. Sakaki, T. Noda, K. Hirakawa, M. Tanaka, and T. Matsusue, Appl. Phys. Lett. **51**, 1934 (1987).